

# Antibiotic Cross-linked Micelles with Reduced Toxicity for Multidrug-Resistant Bacterial Sepsis Treatment

Xingyue Yang, He Ren, Hong Zhang, Gengqi Liu, Zhen Jiang, Qian Qiu, Cui Yu, Niren Murthy, Kun Zhao,\* Jonathan F. Lovell,\* and Yumiao Zhang\*



Cite This: <https://dx.doi.org/10.1021/acsami.0c21459>



Read Online

ACCESS |



Metrics & More



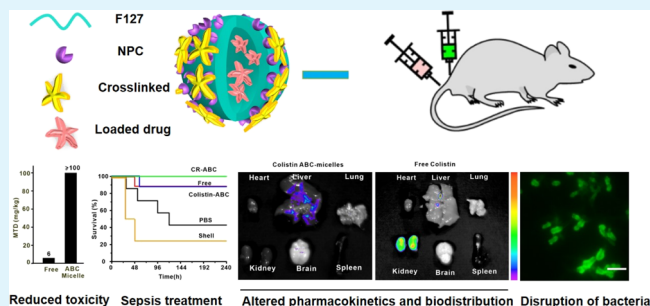
Article Recommendations



Supporting Information

**ABSTRACT:** One potential approach to address the rising threat of antibiotic resistance is through novel formulations of established drugs. We designed antibiotic cross-linked micelles (ABC-micelles) by cross-linking the Pluronic F127 block copolymers with an antibiotic itself, via a novel one-pot synthesis in aqueous solution. ABC-micelles enhanced antibiotic encapsulation while also reducing systemic toxicity in mice. Using colistin, a hydrophilic, potent "last-resort" antibiotic, ABC-micelle encapsulation yield was 80%, with good storage stability. ABC-micelles exhibited an improved safety profile, with a maximum tolerated dose of over 100 mg/kg colistin in mice, at least 16 times higher than the free drug. Colistin-induced nephrotoxicity and neurotoxicity were reduced in ABC-micelles by 10–50-fold. Despite reduced toxicity, ABC-micelles preserved bactericidal activity, and the clinically relevant combination of colistin and rifampicin (co-loaded in the micelles) showed a synergistic antimicrobial effect against antibiotic-resistant strains of *Escherichia coli*, *Pseudomonas aeruginosa*, and *Acinetobacter baumannii*. In a mouse model of sepsis, colistin ABC-micelles showed equivalent efficacy as free colistin but with a substantially higher therapeutic index. Microscopic single-cell imaging of bacteria revealed that ABC-micelles could kill bacteria in a more rapid manner with distinct cell membrane disruption, possibly reflecting a different antimicrobial mechanism from free colistin. This work shows the potential of drug cross-linked micelles as a new class of biomaterials formed from existing antibiotics and represents a new and generalized approach for formulating amine-containing drugs.

**KEYWORDS:** Drug cross-linked micelles, antibiotics, nephrotoxicity, neurotoxicity, sepsis



Reduced toxicity Sepsis treatment Altered pharmacokinetics and biodistribution Disruption of bacteria

## INTRODUCTION

Bacterial infections are a serious threat to global public healthcare, causing millions of deaths annually.<sup>1</sup> Gram-negative pathogens are particularly prone to cause serious infections such as pneumonia,<sup>2,3</sup> blood stream infections,<sup>4</sup> urinary tract infections,<sup>5</sup> and wound infections.<sup>6</sup> To treat these diseases, a wide variety of antibacterial agents have been developed;<sup>7–12</sup> however, the overuse of antibiotics has given rise to drug resistance, representing a looming public health crisis. The World Health Organization designated carbapenem-resistant *Enterobacteriaceae*, *Acinetobacter baumannii* and *Pseudomonas aeruginosa* to be the most critical pathogens.<sup>13</sup>

The lack of new antibiotics for the treatment of multidrug-resistant Gram-negative bacteria has led to the revival in the use of polymyxin (Polymyxin E; colistin).<sup>14</sup> Carbapenem-resistant bacteria isolates have been found to remain highly susceptible to colistin,<sup>15,16</sup> although there have been reports of colistin-resistant isolates.<sup>17</sup> In spite of its strong antibiotic properties, nephrotoxicity and neurotoxicity induced by colistin have been a central problem that is dose limiting.<sup>18,19</sup> Its potential for inducing serious side effects has relegated colistin to a drug of last resort. Structurally, each colistin has five amines and one

hydrophobic tail that can bind and disrupt the outer membrane of bacteria.<sup>20,21</sup> The amine-rich structure also gives rise to its clinical side-effects manifested as renal failure and tubular necrosis,<sup>22</sup> increased oxidative stress,<sup>23</sup> injured mitochondrial function,<sup>24</sup> and even respiratory arrest.<sup>25</sup>

To address colistin toxicity, several strategies have been developed. A modified formulation of colistin for parenteral administration is colistin methanesulfonate (CMS), which reversibly masks the colistin amines.<sup>26</sup> CMS is not stable so that it usually exists as a mixture of several methanesulfonated derivatives,<sup>27</sup> complicating dosage quantification,<sup>28–30</sup> Alternatively, polymer conjugates,<sup>31–33</sup> micelle conjugates,<sup>34</sup> silica nanoparticles,<sup>35</sup> quantum dots,<sup>36</sup> polymeric nanoparticles,<sup>37,38</sup> and lipid nanoparticles<sup>39</sup> have been proposed. However, these approaches typically include large amounts of novel, exogenous

**Received:** December 3, 2020

**Accepted:** February 9, 2021

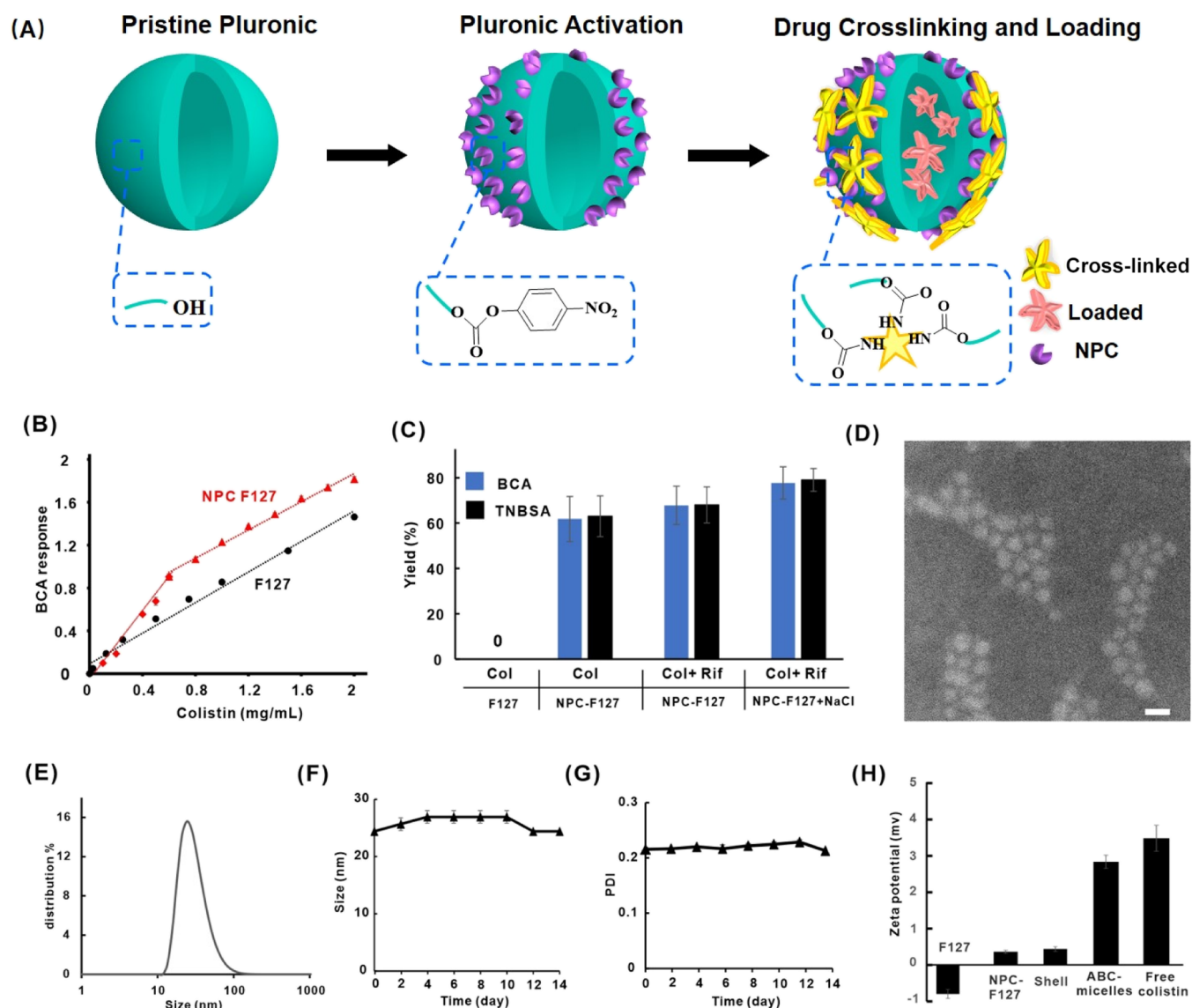


**Figure 1.** Preparation and characterization of antibiotic cross-linked micelles (ABC micelles). (A) Schematic of the formation of colistin ABC-micelles. The terminal hydroxyl group of pristine Pluronic was first activated by NPC and then cross-linked by colistin. Free colistin was encapsulated in drug cross-linked micelles. (B) BCA assays for NPC F127 and regular F127 aqueous solution with the addition of free colistin. For NPC activated F127 (red line), the higher slope indicated formation of new peptide bonds because of the reaction between colistin and NPC group. After the NPCs were completely cross-linked by colistin, the slope of the fitted line decreased back to the same value as regular F127. (C) Subject to centrifugal filtration with membrane MWCO of 100,000, colistin drug retentions are about 0, 62, 68, and 79% for regular F127, colistin ABC-micelles, colistin-rifampicin ABC-micelles (no salt), and colistin-rifampicin ABC-micelles (0.5 molar salt), respectively, by using both the BCA method (for peptide bond measurement) and the TNBSA method (for free amine measurement). (D) TEM images of colistin ABC-micelles. Scale bar: 20 nm. (E) DLS measurement of colistin-rifampicin ABC-micelles. (F) Size and (G) PDI stability of colistin-rifampicin ABC-micelles during storage at 4 °C. (H) Zeta potential values of regular 5% (w/v) Pluronic F127 aqueous solution, 5% (w/v) NPC-F127 aqueous solution, shell of ABC-micelles without colistin encapsulated inside micelles, colistin ABC-micelles, and 1 mg/mL free colistin aqueous solution.

components that may complicate clinical development. Alternatively, adjuvant drugs have been co-administered along with colistin to ameliorate nephrotoxicity and neurotoxicity, including *N*-acetylcysteine,<sup>18</sup> methionine,<sup>40</sup> gelofusine,<sup>41</sup> lycopene,<sup>42</sup> ascorbic acid,<sup>43</sup> curcumin,<sup>44</sup> and cytochrome C.<sup>45</sup> However, the introduction of two separate drug components, as well as determining their respective optimal doses and administration timing, complicates drug development.

Taking the aforementioned points into consideration, a simple and stable colistin formulation with an improved safety profile, while maintaining antibacterial efficacy could be a preferred option. Herein, we report a simple method to use the

amine-containing antibiotic itself to cross-link the FDA-approved block copolymer, Pluronic F127,<sup>46–48</sup> to seal the drug inside antibiotic cross-linked micelles (termed ABC-micelles). Previously, we developed a novel “surfactant-stripped” micelle system for hydrophobic cargos, which can partition in the core of Pluronic micelles owing to hydrophobic–hydrophobic interaction.<sup>49</sup> Given that colistin is not hydrophobic ( $\log P = -1.3$ , Alog *P*s), this prior approach is not viable. To make stable colistin micelles, in this work, we outline an approach in which colistin itself is used to cross-link and encapsulate in micelles. Owing to the temperature-sensitive micellization of Pluronic, free drugs and loosely bound

**Table 1. Minimum Inhibitory Concentrations ( $\mu\text{g}/\text{mL}$ ) of Various Colistin Formations<sup>a</sup>**

bacteria isolates	free colistin	colistin ABC-micelles	rifampicin Micelles	colistin-rifampicin ABC-micelles	FICI <sup>b</sup>
<i>E. coli</i>	2	5	4	1	0.23
MDR <i>E. coli</i>	4	8	8	2	0.29
<i>P. aeruginosa</i>	4	12	16	4	0.36
<i>A. baumannii</i>	4	14	2	$\leq 1$	$\leq 0.32$

<sup>a</sup>MIC values indicate the concentrations of colistin; refer to Figures S4–S6 for more details. ( $n = 3$ ). <sup>b</sup>FICI < 0.5 indicates the synergistic effect between colistin and rifampicin, see method for the calculation.

excipients can then be stripped away when subject to centrifugal filtration at low temperatures, leaving behind concentrated and purified colistin ABC-micelles. Colistin ABC-micelles showed a significantly improved safety profile while preserving antimicrobial potency.

## RESULTS AND DISCUSSION

**Generation of Drug Cross-linked Micelles with Reduced Toxicity.** The terminal hydroxyl group on Pluronic F127 was activated with *p*-nitrophenyl chloroformate (NPC) (termed NPC-F127, see its NMR spectrum in Figure S1) for the reaction with the amine groups of colistin. As such, a part of colistin was cross-linked with micelles, sealing the rest of colistin within Pluronic micelles (Figure 1A). Owing to the temperature sensitivity of Pluronic micellization, unreacted Pluronic and loosely bound surfactant were dissociated to unimers at a low temperature ( $4\text{ }^{\circ}\text{C}$ ), which, together with unloaded and uncross-linked colistin, could be purified by low-temperature centrifugal filtration, leaving behind purified ABC-micelles with a high concentration. We categorized and characterized colistin by loaded amines as free drug or reacted amines as a cross-linking shell.

**Characterization of ABC Micelles.** We first assessed the colistin content within ABC micelles. Colistin, a polypeptide, is detectable with the biconchonic acid assay (BCA).<sup>50</sup> An independent 2,4,6-trinitrobenzenesulfonic acid (TNBSA)-based assay was used for the measurement of free amines, which are present on colistin. As shown in Figure 1B, increasing concentrations of colistin in 5% (w/v) regular F127 resulted in a linear BCA response for regular F127, which reflects the increasing colistin peptide content. However, for the NPC-F127 micelles, colistin addition resulted in a more rapid increase of the peptide bond content than in standard F127 micelles. This suggests that the NPC-modified micelles were reacted with colistin because this cross-linking process generates additional peptide bonds. This phenomenon reached a saturation point at 0.7 mg (in 0.5 mL 5% NPC-F127). Then, the increase rate was almost the same as regular F127, indicating that no more peptide bonds from the reaction between the colistin and NPC group were generated. When a sufficient amount of colistin was cross-linked or conjugated on the surface of NPC-F127 micelles, hydrophilic colistin was able to be loaded in ABC-micelles. As shown in Figure 1C, subject to centrifugal filtration (with 100,000 Da molecular weight cut-off membranes), unactivated F127 micelles could not form stable micelles, leading to complete drug loss, whereas the cross-linking approach increased the yield of colistin micelles from 0 to about 62%. Importantly, the one-pot cross-linking process could happen rapidly in aqueous solution (within several minutes, as shown in Figure S2). For the purpose of developing a powerful antibacterial effect, rifampicin was also co-loaded along with colistin in the ABC micelles, as this combination has previously been shown to be effective against drug-resistant strains.<sup>51</sup> The

addition of rifampicin slightly increased the encapsulation yield of colistin (68%), which may have been because of co-loading effects that we have shown can stabilize cargo in F127 micelles.<sup>49</sup> The addition of 0.5 molar NaCl could further increase the yield (79%, Figure 1C) and the stability of the partition of colistin in the shell (Figure S3) possibly due to the salt altering the polarity of the solvent leading to modulated partitioning in micelles, as we previously reported.<sup>49</sup> The loading yield in the ABC micelles were similar when assessed by either the BCA or TNBSA method. Uniform nanoparticles with a size of 20–25 nm are revealed by TEM and DLS, as shown in Figure 1D,E. During a period of 2 weeks, the size remained unchanged with a low value of PDI, as shown in Figure 1F,G. As shown in Figure 1H, similar to F127 and NPC-F127 micelles, the shell of ABC-micelles is almost neutral because all amines were masked with the NPC group. By contrast, with the addition of more colistin drugs, colistin ABC-micelles have slightly more positive charges because of some of the five amine groups on colistin molecules were not completely reacted with NPC. Other detailed physical parameters of colistin-rifampicin ABC-micelles are summarized in Table S1.

**Minimum Inhibitory Concentrations (MICs).** First, we found that Pluronic F127 itself had no antimicrobial effect even at concentrations up to 10 mg/mL (Figure S6). Next, we evaluated the antimicrobial efficacy of ABC-micelles by measuring minimum inhibitory concentrations (MICs) against several drug-resistant bacteria strains by checkerboard dilution (Table 1; Figures S4–S5). For *Escherichia coli*, free colistin and free rifampicin had a MIC of 2 and 4  $\mu\text{g}/\text{mL}$ , respectively. Colistin ABC-micelles and rifampicin Pluronic micelles had a 2.5-fold higher (5  $\mu\text{g}/\text{mL}$ ) or equivalent (4  $\mu\text{g}/\text{mL}$ ) MICs, respectively. However, the combination of 1  $\mu\text{g}/\text{mL}$  colistin and 0.128  $\mu\text{g}/\text{mL}$  rifampicin in ABC-micelles (shown in red) showed the lowest MIC value of 1  $\mu\text{g}/\text{mL}$ . The fractional inhibitory concentration index (FICI) value was calculated to be less than 0.3, indicating a synergistic antibacterial efficacy of the two antibiotics against *E. coli*. The synergistic efficacy was observed in the range of 0.128–1.44  $\mu\text{g}/\text{mL}$  rifampicin in combination with 1  $\mu\text{g}/\text{mL}$  colistin (Figure S4B,C). This synergistic antibacterial effect in ABC micelles was further confirmed in multidrug-resistant *E. coli* (imipenem resistant and ertapenem resistant), *P. aeruginosa* and *Acinetobacter baumannii* (Table 1 and Figure S5A–C). For these studies, we used loaded colistin for dose calculation because up to 512  $\mu\text{g}/\text{mL}$  cross-linked colistin (shell) had no antibacterial effect considering amines are primarily responsible for killing bacteria but were masked by the NPC group (Figure S7). Furthermore, we evaluated the long-term stability of colistin used for cross-linking (shell). As shown in Figure S8, the shell remained stable within one week when subjected to dialysis in PBS containing 5% fetal bovine serum (FBS). We also measured minimum bactericidal concentrations (MBCs) of free colistin and ABC-micelles

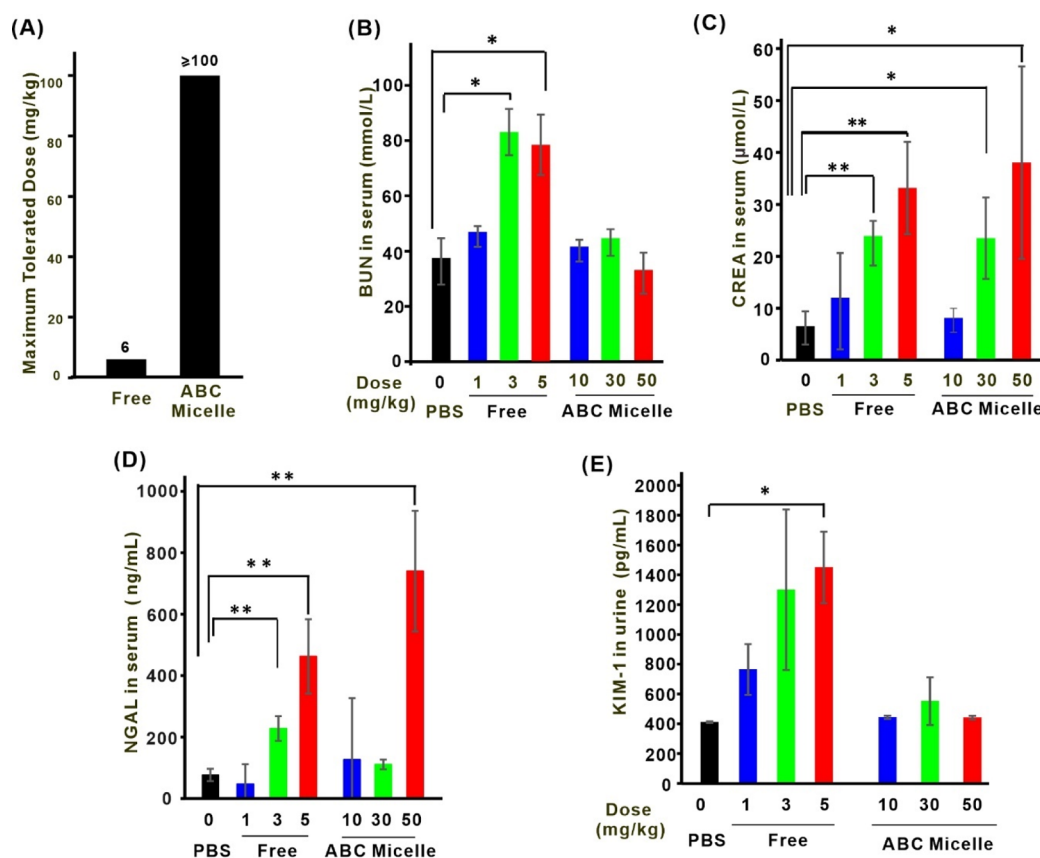


**Figure 2.** Reduced nephrotoxicity of colistin ABC micelles compared to the free drug. (A) MTD of free colistin and colistin ABC-micelles.  $n = 5$  for Free and colistin ABC-micelle groups. The concentration of (B) BUN in the serum;  $n = 3-4$  independent mice for each group, respectively. (C) CREA in the serum;  $n = 4-5$  for each group, respectively. (D) Lipocalin-2 (NGAL) in the serum.  $n = 3-4$  for each group. (E) KIM-1 in urine after the intravenous injection of formulations at indicated doses.  $n = 3-4$  for each group. For A, one single dose was given; or B-F, formulations were administered daily for seven successive days and mice were sacrificed 12 h after the last injection. Control mice were treated with PBS. (One-way analysis of variance was used for significant difference analysis,  $*P < 0.05$ ,  $**P < 0.01$ ,  $***P < 0.001$ ).

against various bacteria isolates, as shown in Table S2, which were not significantly different from the MICs.

**Toxicity Evaluation in Vivo.** Next, we evaluated the in vivo toxicity of colistin ABC-micelles including the maximum tolerated dose (MTD), nephrotoxicity, and neurotoxicity. As Figure 2A and Table S3 demonstrate, when mice were given one single intravenous injection, the MTD of free colistin was close to 6 mg/kg, and further increase in dose caused the death of at least one mouse within 24 h. In contrast, a dose of over 100 mg/kg of colistin ABC micelles was tolerated, suggesting at least a 16-fold greater MTD compared to free colistin. Then, we evaluated chronic nephrotoxicity. Different cohorts of mice were given different doses every day for seven successive days. Colistin-induced renal injury is related with the filter capability of renal glomeruli and increased permeability of the tubular epithelial cell membrane. Drug elimination by renal tubular cells can cause the accumulation of colistin and re-absorption by tubules.<sup>42,52</sup> Blood urea nitrogen (BUN) and creatinine (CREA) are two biomarkers commonly used for the evaluation of glomeruli damage. For groups receiving free colistin, the doses of 1, 3, and 5 mg/kg were selected. For the colistin ABC-micelle group, we increased the doses by ten times to 10 mg/kg, 30 mg/kg, and 50 mg/kg. As shown in Figure 2B, mice in the 3 mg/kg free colistin group show an elevated level of BUN, whereas for the ABC-micelle group, even at the highest dose of 50 mg/kg, ABC-micelles did not give rise to significantly increased levels of BUN in the serum. Similarly, as shown in Figure 2C, mice in the

3 mg/kg free colistin group showed elevated levels of CREA, whereas mice in the 10 mg/kg ABC-micelle group did not. In addition, we also assessed the neutrophil gelatinase-associated lipocalin (NGAL) level in serum and kidney injury molecule-1 (KIM-1) level in urine, which are more sensitive and specific biomarkers for kidney injury diagnosis.<sup>53,54</sup> As shown in Figure 2, 3 mg/kg free colistin induced significantly elevated NGAL levels in the serum, whereas 30 mg/kg colistin ABC-micelles did not cause any difference compared to the control group. Similarly, as shown in Figures 2E, 5 mg/kg free colistin induced significantly higher levels of KIM-1 in urine, whereas doses as high as 50 mg/kg colistin ABC-micelles did not induce any difference compared to the control group. We also examined the histological structure of the kidney of mice administered 3 mg/kg free colistin or 30 mg/kg colistin ABC-micelles for seven days, as shown in Figure S9. One out of 3 mice in the free colistin group was discovered to have degeneration in the curved pipe, but for the colistin ABC-micelle group given 10 times higher dosage, one out of 3 mice was found to have local inflammatory cells slightly infiltrating into the stroma. These results indicate that colistin ABC-micelles reduced nephrotoxicity by at least 10–50-fold.

Colistin-induced neurotoxicity is usually mild and resolves after the treatment discontinues. However, some non-negligible clinical manifestations of colistin associated neurotoxicity still exist including paresthesia and ataxia. The neurotoxicity can be attributed to colistin accumulation in central nervous systems,

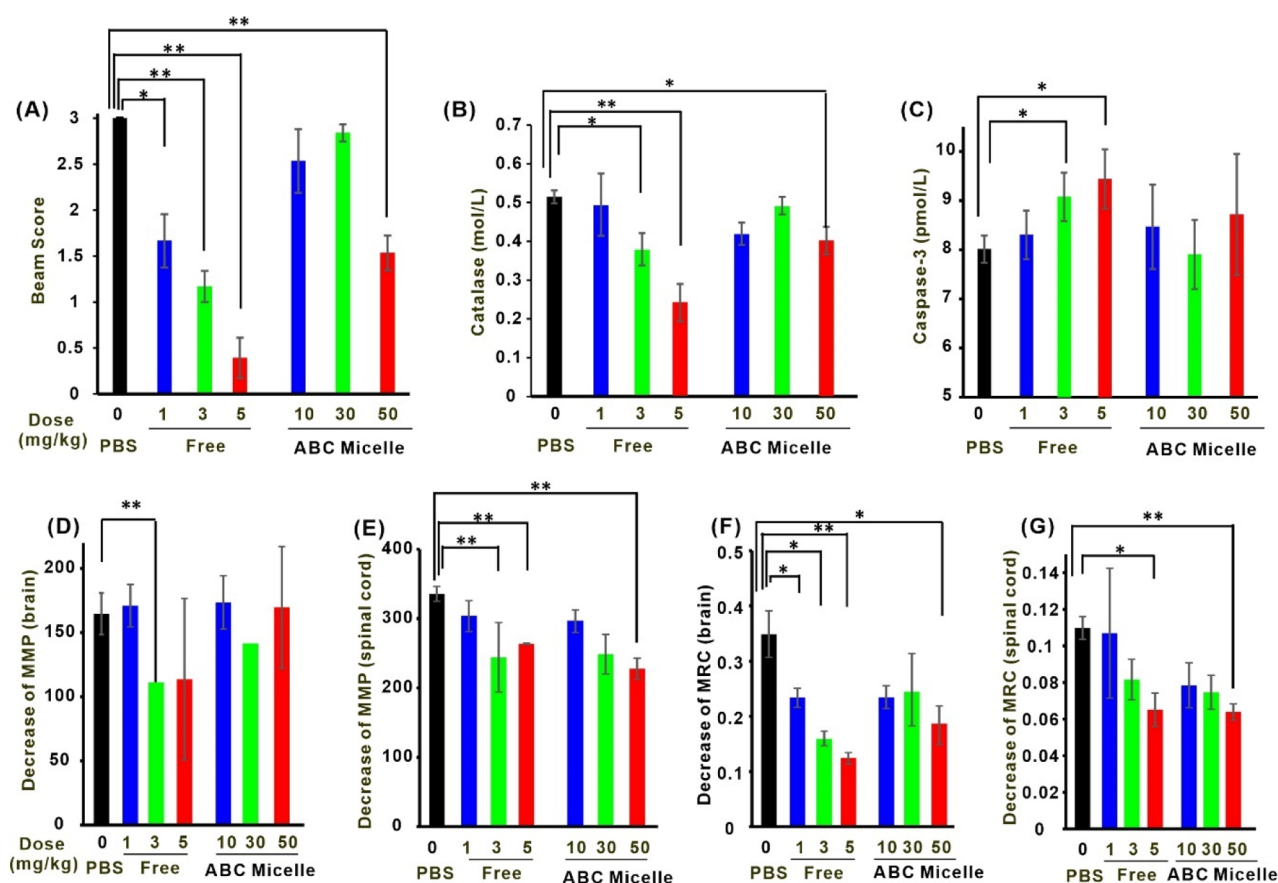


**Figure 3.** Reduced neurotoxicity of colistin ABC micelles compared to the free drug. Mice were injected intravenously with different formulations at the indicated doses for one dose per day for seven successive days, and mice were euthanized 24 h after last injection. PBS group ( $n = 3$ ) was given PBS. (A) Beam score of mice. Score was calculated by measuring the distance that mice were able to traverse across the narrow beam without falling.  $n = 4, 4, 5, 5, 5, 5$  for free colistin-3, colistin ABC-30, free colistin-1, free colistin-5, colistin ABC-10, and colistin ABC-50, respectively. Concentration of (B) catalase and (C) caspase-3 of mice in brain cerebrum 12 h after the last injection.  $n = 3$  for PBS group and  $n = 4$  for 1, 3, 5 mg/kg free colistin and 10, 30, and 50 colistin ABC-micelles. Decrease of mitochondrial membrane potential, MMP in (D) brain and (E) in spinal cord 12 h after the last injection. Decrease of activity of the mitochondrial respiratory chain (MRC), (F) in brain mitochondria and (G) in spinal cord 12 h after the last injection.  $n = 4$  except 50 mg/kg colistin ABC-micelles group in the spinal cord ( $n = 5$ ). One-way analysis of variance was used to analyze significant difference, all groups were compared with the PBS group. The other groups not noted were not statistically different. \* $P < 0.05$ , \*\* $P < 0.01$ , and \*\*\* $P < 0.001$ .

manifested as elevated oxidative stress or mitochondrial dysfunction.<sup>24,55,56</sup> To assess the neurotoxic potential, mice were divided into three groups and given PBS; free colistin (1, 3, or 5 mg/kg) or colistin ABC-micelles (10, 30 or 50 mg/kg colistin). First, we investigated the neurobehavioral performance by narrow beam test.<sup>19,57</sup> As shown in Figure 3A, mice treated with free colistin show significantly impaired movement especially at the doses of 3 and 5 mg/kg. However, mice given 30 mg/kg colistin ABC-micelles could walk as normally as control mice. Next, we studied the oxidative stress level when mice were treated with free colistin or colistin ABC-micelles. Catalase, an antioxidant enzyme that can degrade toxic oxidative species, was investigated.<sup>58,59</sup> Mice treated with 3 mg/kg showed significantly lower levels of catalase in the cerebrum homogenate compared to PBS mice; however, up to 30 mg/kg colistin ABC-micelles had an unchanged level of catalase (Figure 3B), which suggests that ABC-micelles reduced neurotoxicity with reduced oxidative stress by at least 10-fold. Besides the production of reactive oxygen species, colistin-induced neurotoxicity also involves the activation of caspase-3, -8, -9, and mitochondrial pathways. As shown in Figure 3C, colistin ABC-micelles suppress the increase of caspase-3 by at least 10 times relative to the free drug. Then, we examined the mitochondrial function

when mice were treated by different formulations and doses. As shown in Figure 3D–G, free colistin of 1–3 mg/kg affected the mitochondrial membrane potential and activities of the mitochondrial respiratory chain in the cerebrum and spinal cord. However, the dose of up to 30 mg/kg colistin ABC-micelles did not obviously impact for mitochondrial functions in either the cerebrum or spinal cord. Also, 30 mg/kg colistin ABC-micelles did not induce a noticeable inflammatory response or damages to the brain by the histology examination (Figure S10). These results indicate that colistin ABC-micelles reduced neurotoxicity by at least 10–50-fold compared to the free drug. Taken together, 30 mg/kg colistin ABC-micelles appear to be a safe dose for intravenous injection on mice, at least within the one-week observational period. Furthermore, we also examined the toxicity of 30 mg/kg colistin ABC-micelles within a two-week period and found no significant nephrotoxicity (Figure S11A). The reduced nephrotoxicity of colistin ABC-micelles is likely because of the changed clearance pathway, but liver toxicity was not seen either, as shown in Figure S11B. In the following antimicrobial efficacy in vivo experiment discussed below, only 3 mg/kg of colistin ABC-micelles were used but with rifampicin co-loaded. Co-loading rifampicin did not induce additional nephrotoxicity, as shown in Figure S12.

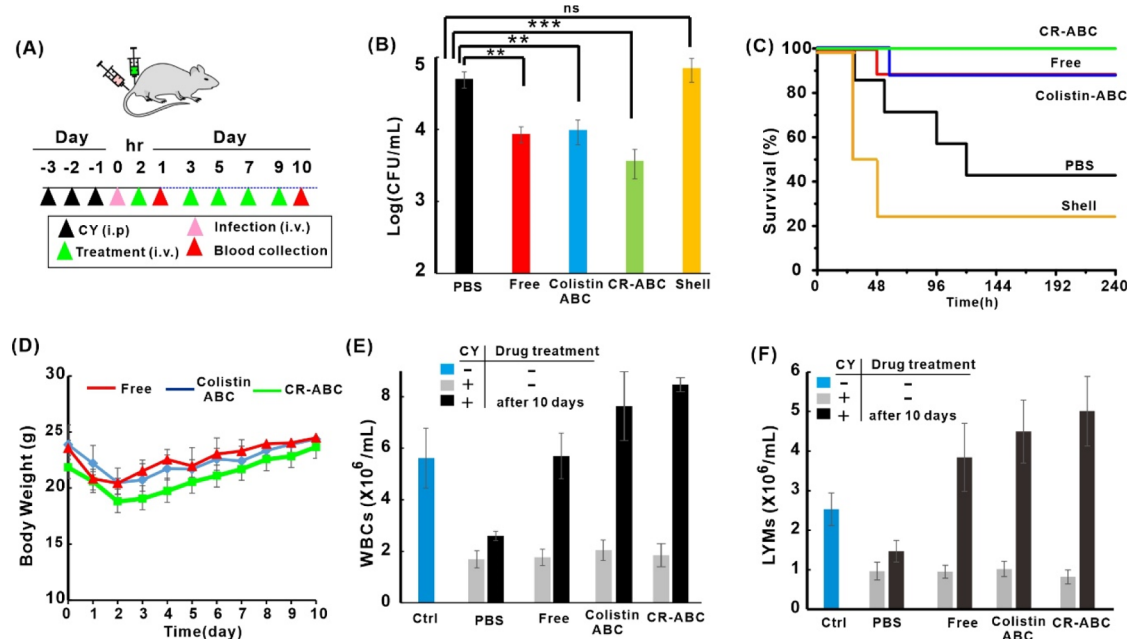


**Figure 4.** Treatment of sepsis by colistin-rifampicin ABC-micelles (A) Schematic of experimental design. Mice were given cyclophosphamide (CY) intraperitoneally for three consecutive days, then different formulations including free colistin, colistin ABC-micelles, colistin-rifampicin ABC-micelles (CR-ABCs) or shell were administered 2 h after microbial infection. Blood was collected for bacteria counting 1 day after drug treatment. (B) Bacterial CFU recovered from blood 24 h after treatment by different colistin formulations.  $n = 6, 7, 7, 8,$  and  $3$  for PBS, Free, Colistin ABC-micelles, CR-ABC-micelles, and shell groups, respectively. (C) Survival rates for different groups.  $n = 7-8$  per group. (D) Body weight changes within 10 days. (E) WBCs and (F) LYMs after 10 days with the treatment scheme, as shown in Figure 4A. Level of WBCs, LYMs were recovered fully after treatment for free colistin and ABC groups but not for the PBS group. One-way analysis of variance was used to analyze significant difference, all groups were compared with PBS,  $*P < 0.05$ ,  $**P < 0.01$ ,  $***P < 0.001$ .

### Antibacterial Efficacy in Vivo for Sepsis Treatment.

Encouraged by the safety profile and in vitro antibacterial activity of ABC-micelles, we next evaluated its therapeutic effects in a murine model of sepsis. In this model, mice were given cyclophosphamide (CY) intraperitoneally for three consecutive days, mimicking an immune-compromised condition with decreased white blood cells (WBCs) and lymphocytes (LYMs). As shown in Figure 4A, in the sepsis model, mice were infected by multidrug-resistant *E. coli*. Two hours later, mice were given PBS or treated with 3 mg/kg colistin, either as free colistin, colistin ABC-micelles, or colistin-rifampicin ABC-micelles (CR-ABCs). Bacterial colony forming unites (CFUs) were measured in mouse blood 24 h after infection. As shown in Figure 4B, Colistin-ABCs significantly reduced bacterial burden in blood, as did free colistin. Because of the addition of rifampicin and its synergistic effect with colistin, CR-ABCs showed even better treatment efficacy. Next, we assessed the bacterial burden in major organs after treatment by ABC-micelles. As shown in Figure S13A, free colistin and colistin-ABC micelles significantly relieved the bacterial burden (CFU count) in kidneys by about 2 orders of magnitude, whereas co-loaded CR-ABC micelles alleviated the CFUs of major organs by about 2–3 orders of magnitude especially in the kidney, spleen, and lung. In addition, after infection, the inflammatory response might also induce organ damage. Therefore, we measured the concentration of interleukin-6 (IL-6) in serum after bacteria challenge. As shown in Figure S13B, treatment by CR-ABC micelles as well as colistin ABC-micelles and free colistin, but not PBS, could significantly ameliorate the inflammatory response nearly to normal levels (mice with no bacteria challenge). The drug cross-linked shell group without colistin inside did not show an antibacterial effect, similar to the in vitro results, as

shown in Figure S7. Both free colistin and colistin-ABC micelle groups improved the survival of mice within 10 days and no death were observed in the CR-ABC group compared to the PBS control group that had less than 50% survival rate (Figure 4C).<sup>60</sup> Importantly, after 10 days, the body weight, WBCs and LYMs fully recovered for free and ABC groups, but not the surviving mice in the PBS group, which had lower WBC and LYM counts, along with the symptoms of slow movement and piloerection (Figure 4D–F).

In order to shed light on the safety profile and strong antibacterial potency of ABC-micelles, pharmacokinetics and biodistribution were also assessed. To accurately measure the concentration of colistin in tissues, colistin was fluorescently labeled by fluorescein isothiocyanate (FITC) so that concentrations as low as  $0.05 \mu\text{g/mL}$  could be detectable by fluorescence measurement, at least 500 times higher sensitivity than the BCA assay or HPLC method (Figure S14). As demonstrated in Figure 5B, ABC-micelles increased the half-life of colistin in blood from 40 min to over 2 h. Free colistin tends to be accumulated in the kidney to cause nephrotoxicity but using this cross-linking strategy, the kidney accumulation after 24 h was significantly reduced (Figure 5C,D) and ABC-micelles were distributed more in the liver and spleen (Figure 5C,D). It can be concluded that compared with free drug form, colistin loaded in ABC-micelles exhibited different pharmacokinetic behaviors and biodistributions in vivo, leading to reduced nephrotoxicity and neurotoxicity.

Bacterial behaviors monitored by microscopic single-cell imaging. To further investigate the antimicrobial mechanism of ABC-micelles, bacterial behaviors at the single-cell level were also monitored in the presence of free colistin and colistin ABC-micelles with the same colistin concentration ( $16 \mu\text{g/mL}$ ) using

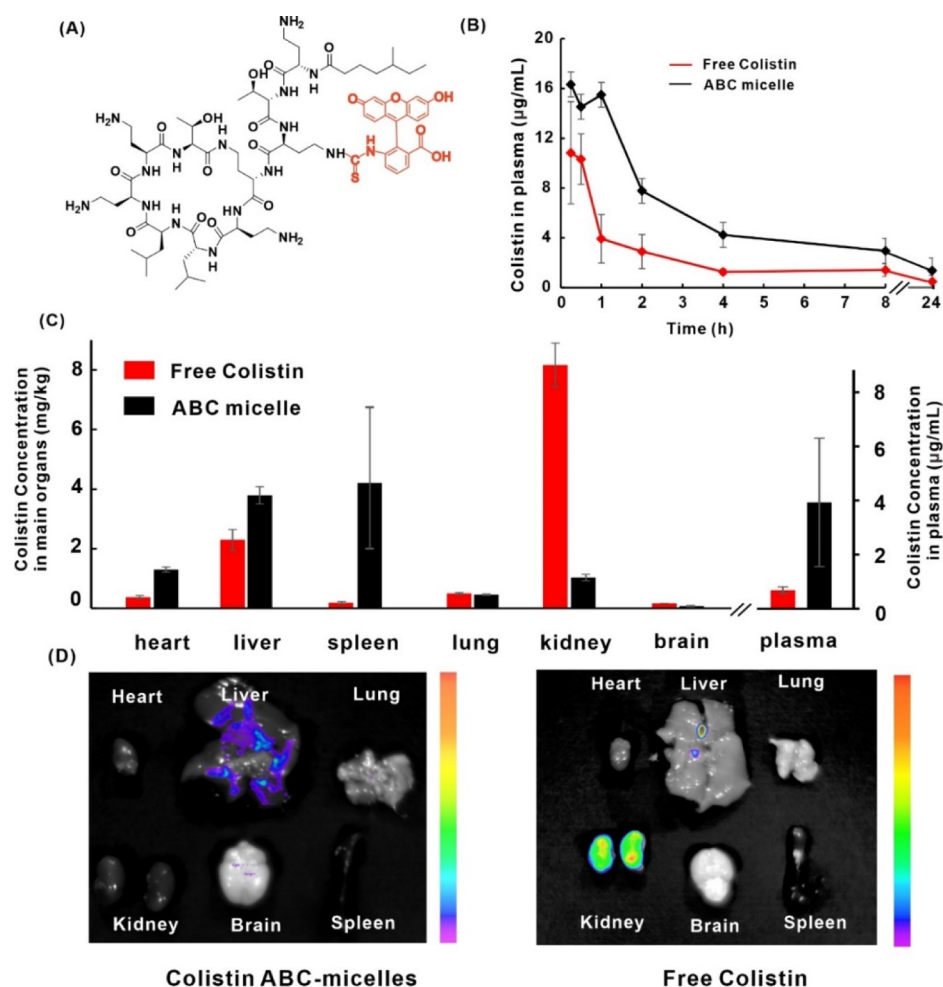


**Figure 5.** Pharmacokinetics and biodistribution of colistin ABC-micelles (A) chemical structure of FITC-labeled colistin. (B) Blood levels of free colistin and colistin ABC-micelles. (C) Biodistribution of free colistin and colistin ABC-micelles 24 h after injection.  $n = 3$  independent mice for half-life and biodistribution. (D) Representative fluorescent images of main organs including heart, liver, spleen, lung, kidney, and brain 24 h after injection of colistin ABC-micelles and free colistin.

bacterial tracking techniques.<sup>61</sup> As shown in [Supplementary Movie 1](#), we found that  $16 \mu\text{g/mL}$  colistin ABC-micelles induced significant morphology changes in *P. aeruginosa* within 2 min of exposure. It was observed that after the addition of colistin ABC-micelles, blebs first appeared somewhere on the cell body, and then grew bigger as the bacteria gradually lost shape integrity, which, at the end, led to a flattened lysed cell with rough contours. A similar blebbing phenomenon was observed in *E. coli* when treated by colistin ABC-micelles ([Figure S15](#)). Representative images of bacteria treated with free colistin or colistin ABC-micelles at the indicated time points are shown in [Figure 6A](#). Quantitatively, within 10 min, almost all bacteria underwent the above-described structural disruption by colistin ABC-micelles, whereas, no such disrupted cells were observed in the free colistin group ([Figure 6B](#)). By contrast, when treated by  $16 \mu\text{g/mL}$  of free colistin for 10 min, there were still a significant part of cells with intact cell membranes indicated by the green only fluorescence when stained with the live/dead staining assay ([Figure S16](#)), but later after 90 min, most bacteria lost membrane integrity indicated by the red fluorescence, implying the death of bacteria ([Figure S16](#)). The morphology of cells treated by  $16 \mu\text{g/mL}$  of free colistin was quite different from that treated by ABC-micelles. After 2 h incubation in  $16 \mu\text{g/mL}$  free colistin, cells were only observed to be slightly shortened in

length ([Figure 6A,C](#)) and no dividing were observed during the incubation time, suggesting that  $16 \mu\text{g/mL}$  colistin inhibited the cell growth but without causing a significant cell morphology change ([Movie 2](#)). These observations of free colistin are consistent with the earlier results using an atomic force microscope,<sup>62</sup> although a few previous studies showed that *P. aeruginosa* and *E. coli* could induce slight cracks of the cell envelopes but without significant morphology collapse.<sup>63</sup>

One common mechanism of action of colistin is that it can interact strongly with phospholipids because of its amphipathic and cationic nature, and thus can disrupt the structure of cell membranes.<sup>64</sup> In this work, both free colistin and colistin ABC-micelles are observed to be attached to the cell bodies presumably because of the electrostatic interactions ([Figure 6A](#)). In addition, the shell only ABC-micelles without a core load are also slightly positively charged and were attached to the cell bodies although it seemed no drug was immediately released into bacteria ([Figure 6D](#)). However, the local concentrations of active colistin molecules for free and ABC-micelle forms are likely to be different. Under the same total concentration of active colistin molecules, the colistin ABC-micelles contain a local concentration of active colistin molecules around 3 orders of magnitude higher than the case of free colistin based on geometry calculation.<sup>49,65</sup> Such a high concentration of colistin

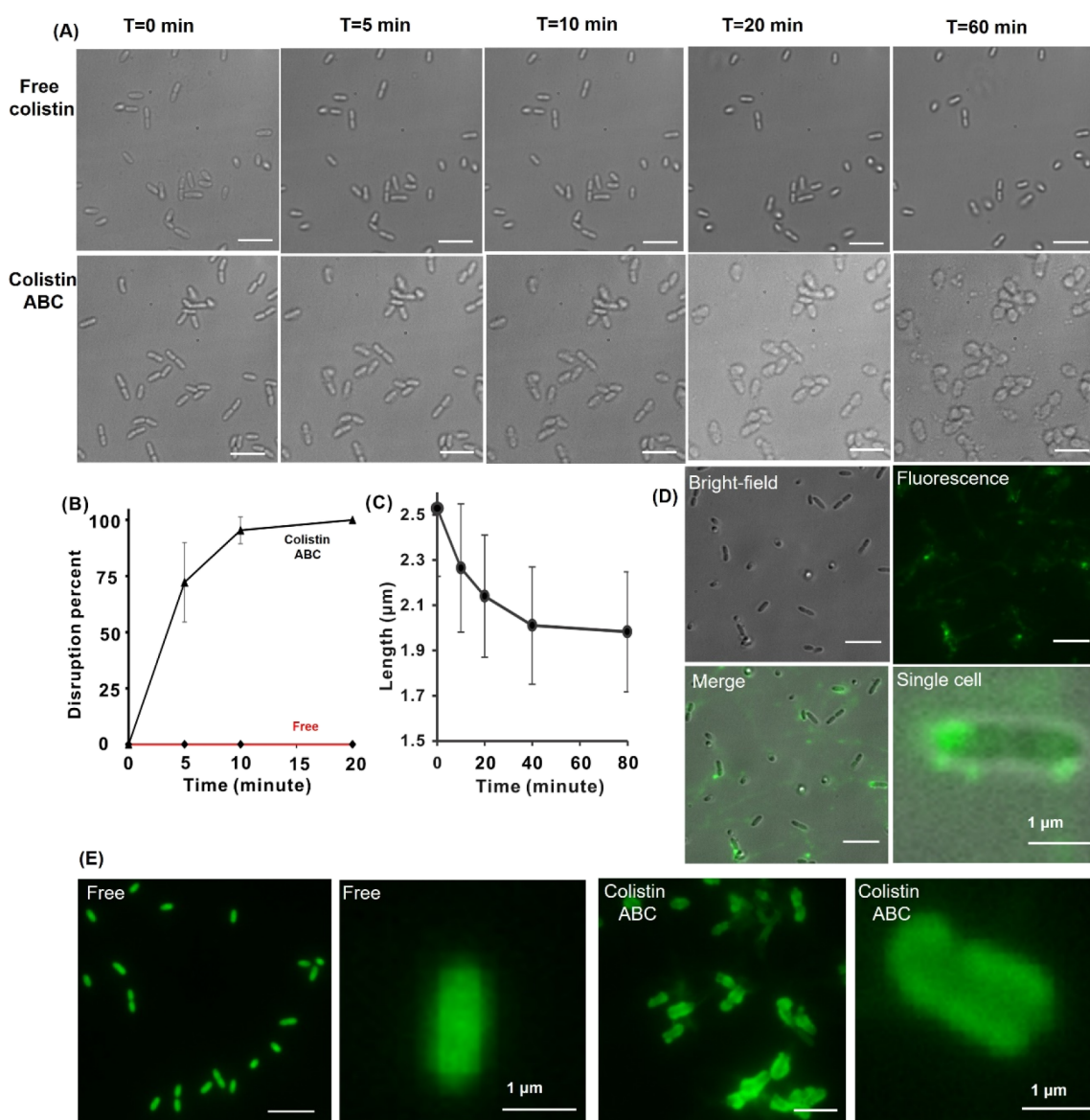


**Figure 6.** Microscopic imaging of *P. aeruginosa* (A) bright-field microscopic images of *P. aeruginosa* treated with 16  $\mu\text{g}/\text{mL}$  drug of free colistin (top) and colistin ABC-micelles (bottom). (B) Disruption of *P. aeruginosa* over time when exposed to 16  $\mu\text{g}/\text{mL}$  colistin ABC-micelles. (C) Length change of bacterial cells treated with 16  $\mu\text{g}/\text{mL}$  free colistin. (D) Microscopic images of *P. aeruginosa* treated with shell of ABC-micelles with no drug inside for 60 min. (E) Fluorescent microscopic images of *P. aeruginosa* after treatment of 16  $\mu\text{g}/\text{mL}$  free colistin or 16  $\mu\text{g}/\text{mL}$  colistin ABC-micelles for 6 min. Scale bars indicated 5  $\mu\text{m}$  unless otherwise noted.

might induce a stronger local interaction with the cell membrane. This not only induces cell death because of the enhanced bactericidal effect but also shortens the incubation time needed to kill bacteria, which can be evidenced by the results using a higher concentration of colistin ABC-micelles (32  $\mu\text{g}/\text{mL}$ ) where the cells are observed to be lysed quickly (within 30 s) even no blebbing appeared (Movie 3). In addition, FITC-labeled colistin in the free form could be evenly distributed in bacteria (Figure 6E), which was also revealed by fluorescent imaging scans at different Z values (Figure S17). However, when treated and stained by colistin ABC-micelle formulation, the surface of bacteria is more fluorescent than its core, indicating that the colistin ABC-micelles were attached to the surface first and colistin then was released into the bacteria. Taken together, colistin ABC-micelles likely exhibit a different antibacterial mechanism from free colistin, although further investigations are

needed for a deeper understanding of the antimicrobial mechanism and whether this mechanism also applies in vivo.

## CONCLUSIONS

Previously, we reported a series of strategies to compact cargo in Pluronic micelles to achieve high cargo-to-excipient molar ratios.<sup>49,65,66</sup> However, this method is not viable for hydrophilic active pharmaceutical ingredients such as colistin. Also, hydrophilic cargos would generally be prone to partition outside polymeric nanoparticles, leading to low encapsulation efficiency. In this study, we introduced the concept of drug cross-linked Pluronic micelles. Without introducing additional exogenous cross-linkers, we used amine-containing hydrophilic colistin itself as cross-linker to formulate colistin-cross-linked Pluronic micelles with a high loading efficiency. Notably, this method for making drug cross-linked micelles represents a simple and versatile approach for formulating hydrophobic or hydrophilic

amine-containing drugs and can be explored with a wide range of other active APIs. Colistin is a powerful antibiotic to treat drug-resistant bacterial infections; however, it is limited by its nephrotoxicity and neurotoxicity. Presumably, the ABC strategy changed the interaction of colistin with renal and neural cells by altering the size and pharmacokinetics of colistin. Colistin ABC-micelles reduced the accumulation of colistin in the kidney. Importantly, colistin ABC-micelles retained the antimicrobial efficacy and significantly reduced toxicity compared to the free drug. The antibacterial activity of loaded colistin in ABC-micelles was as effective as the free drug but with a higher therapeutic index. Hydrophobic rifampicin was co-loaded with colistin in ABC-micelles, leading to the synergistic antimicrobial effect. ABC-micelles improved survival in a murine multidrug-resistant bacterial sepsis model and reduced bacterial burden in blood while avoiding systemic toxicity. Microscopic imaging of bacteria enabled the visualization of bacterial killing in real time and ABC-micelles showed a different interaction manner with bacteria compared to free colistin. We conclude that ABC micelles warrant further investigation as a potential treatment option for sepsis.

## EXPERIMENTAL SECTION

**Synthesis of NPC-F127.** Dehydrated Pluronic F127 (10 g) and 1.005 g NPC were dissolved in 30 mL of benzene and 5 mL of benzene, respectively, and then F127 solution was added dropwise into NPC solution. After stirring at 25 °C for 24 h under an argon atmosphere, the solvent was removed by rotary evaporation. Subsequently, the product was dissolved in benzene and precipitated in cold diethyl ether three times. The final product was put in vacuum overnight for further characterization and use.

**Colistin ABC-Micelles and Colistin-Rifampicin ABC-Micelle Formation.** For colistin ABC-micelle preparation, the procedure is the same as colistin-rifampicin ABC-micelles but without adding rifampicin/DMSO solution. For colistin-rifampicin ABC-micelles: first, 2.5 mg of rifampicin was dissolved in 100  $\mu$ L of DMSO, which then was added dropwise to 1 mL of NPC-F127 (5%, w/v) in pH = 9 sodium phosphate buffer solution with 0.5 M sodium chloride. Then, 10 mg of colistin sulfate was dissolved in 100  $\mu$ L of distilled water and then added dropwise to the rifampicin-NPC F127 solution, and the mixture was stirred at room temperature for 3 h. To remove uncross-linked NPC F127, the solution was centrifuged in a centrifugal filtration device with a 100,000 MWCO (Millipore) for at least three times. 0.5 M sodium chloride aqueous solution was added back to the filtration device for the next wash. It also should be noted that drug cross-linking and loading occurred at the same time using this one-pot synthesis because 10 mg (>0.7 mg) of colistin was used for the preparation of colistin ABC-micelles. The yield of colistin loaded into micelles was calculated with the following equation: Colistin yield (%) = (colistin encapsulated in ABC-micelles)/(starting materials of colistin excluding cross-linked colistin as shell)  $\times$  100. The shell in this work was referred to as the cross-linked colistin without free drugs encapsulated inside micelles, which was excluded for calculation of drug contents because it has no antimicrobial potency, as shown in Figures 4B and S7.

For peptide bond quantification of colistin in regular F127 and modified F127, as shown in Figure 1B: 0.1, 0.2, 0.4, 0.6, 0.8, 1, 1.2, 1.4, 1.6, 1.8, 2 mg of colistin were added into sodium phosphate buffer solution (0.1 M, pH = 9) of 0.5 mL NPC-F127 (5%, w/v) and stirred for 3 h at room temperature. The amount of peptide bonds and free amines in colistin were quantified with the BCA method and TNBSA, respectively. The concentrations of rifampicin were determined by measuring the absorbance.

**ABC-Micelle Characterization.** For colistin quantification, both BCA assay (Thermo Fisher) and TNBSA assay (Yinuokai, Beijing, China) were used for peptide bond and free amine measurements according to the protocols provided by commercial kits. Drug dose was calculated using the loaded drug with a shell (crosslinked colistin)

excluded because it has no antimicrobial effect after free amines are masked. Rifampicin was determined by measuring absorption at 474 nm.

To investigate the release of colistin and rifampicin during storage at 4 °C, samples were subjected to ultracentrifugation using filtration device with a 100,000 MWCO (Millipore) three times at the indicated timepoints. Ten times the volume of 0.5 M sodium chloride solution was added back to colistin-NPC-F127 micelles. Then, retentions of colistin were quantified by BCA and TNBSA assays, and rifampicin was quantified by measuring absorption at 474 nm. Freshly made samples were used for all in vitro and in vivo experiments. To investigate the long-term stability of the shell, fluorescently FITC-labeled shell was subject to dialysis against 5% FBS in and outside the dialysis bag with a molecular weight cutoff of 8000–14,000 at 37 °C within one week. The fluorescence in the dialysis bag was measured every day.

**Transmission Electron Microscope and Zeta Potential.** Colistin ABC-micelles were negatively stained using sodium phosphotungstate (1%) and then imaged by a field-emission transmission electron microscopy (JEM-2100F, Japan). Size measurement were carried out using dynamic light scattering with a Nano ZS90 Zetasizer (Malvern Instruments). Zeta potential of colistin ABC-micelles diluted in deionized water was measured by Malvern Zetasizer as well.

**Minimum Inhibitory/Bactericidal Concentration (MIC/MBC).** *E. coli.* (strain CICC 10003) and *MDRE. coli.* (strain ATCC BAA-2452, resistant to imipenem and ertapenem) were purchased from China Center of Industrial Culture Collection (CICC). *P. aeruginosa* (strain PAO1) and *A. baumannii* (strain 17978) were kindly provided by Prof. Kun Zhao's group at Tianjin University (*A. baumannii* strain is a gift from Prof. Wei Hu at Shandong University). The values reported in the MIC table were the concentrations of colistin. Antibacterial susceptibility testing of free colistin, colistin ABC-micelles, rifampicin, rifampicin-F127 micelles, and colistin-rifampicin-ABC micelles was conducted according to Clinical and Laboratory Standards Institute (CLSI) guideline. MIC values of colistin and colistin-formations were determined by the broth microdilution method. Briefly, bacterial cultivated to the logarithmic phase using liquid LB medium at 37 °C with shaking at 220 rpm were adjusted to a turbidity of  $0.5 \pm 0.05$  McFarland and incubated with colistin and colistin-formations (ranging from 256 to 0.25  $\mu$ g colistin/mL based on free amine concentration) overnight at 37 °C. MIC value was read as the lowest concentration of colistin, completely inhibiting the growth of bacterial through visual distinction and absorbance of OD 600 measurement. The relation between absorbance OD 600 and concentration of colistin was plotted and the lowest value that absorbance lower than 0.1 was recorded. For the determination of MBC, the transparent liquids in the plate wells of the MIC experiments after overnight incubation were applied to LB agar plates evenly, followed by further incubation at 37 °C for 16–24 h, the MBC value was recorded as the lowest concentrations of free colistin and colistin ABC-micelles when no bacteria grew on the plates.

**Synergetic Effect of Rifampicin on Colistin ABC-Micelles.** MICs of different formations including free colistin aqueous solution, rifampicin methanol solution, rifampicin F127 micelles, colistin ABC-micelles, and colistin-rifampicin ABC-micelles were measured. Similarly, to encapsulate the rifampicin into colistin ABC-micelles, 2.5, 5, 10, and 12.5 mg of rifampicin were dissolved in 100  $\mu$ L of DMSO and then were added into 1 mL of NPC-F127 solution, respectively. Then, 10 mg of colistin was added into the NPC-F127 solutions. The concentrations of colistin encapsulated in micelles were determined by BCA and TNBSA methods. The concentrations of rifampicin were measured at the absorption of 474 nm. MICs of colistin and rifampicin in colistin-rifampicin ABC-micelle formations were detected using the broth microdilution method based on the colistin concentration and corresponding concentrations of rifampicin was calculated based on the original concentrations and dilution factors. Fractional inhibitory concentration index (FICI) is defined as following formula:  $FICI = MIC \text{ of A in combination} / MIC \text{ of A} + MIC \text{ of B in combination} / MIC \text{ of B}$  ( $FICI \leq 0.5$  was considered as synergy,  $0.5 < FICI \leq 1$  was considered as additive,  $1 < FICI \leq 4$  was considered as indifference,  $FICI > 4$  was considered as antagonism).

To confirm that the shell of colistin ABC-micelles without unmodified free amines has no antibacterial effects, 0.5 mg of colistin sulfate was added into sodium phosphate buffer solution (0.1 M, pH 9) of 0.5 mL of NPC-F127 (5%, w/v) and was stirred at room temperature for 3 h. The TNBSA method was used to verify no presence of free amines. MIC of the shell of colistin ABC-micelles against *E. coli* was measured by broth microdilution method as described above.

**Nephrotoxicity of Free Colistin and Colistin ABC-Micelles in Vivo.** Eight-week-old female CD-1 mice were purchased from Charles River Beijing Co., Ltd (Beijing, China). Animal experiments were performed in accordance with Tianjin University Institutional Animal Care and Use Committee (Protocol number: TJUE-2020-033).

MTD is defined as the maximum dose under which the mice kept alive for at least 2 weeks after drug administration. The mice were intravenously injected with free colistin with 5, 6, 7, 7.5, 8, 9, 9.5, 10, and 15 mg/kg doses through the tail vein ( $n = 3$  or 5). For colistin ABC-micelles, mice were injected with colistin ABC-micelles with 50, 70, 90, 100, and 125 mg/kg through tail vein ( $n = 1$  or 5). See Table S3 for more details.

For renal toxicity and neurotoxicity of colistin and colistin micelles, the mice were divided into PBS, free colistin-1, 3, and 5 mg/kg, and colistin ABC-micelles -10, 30, and 50 mg/kg groups (each group  $n \geq 3$ ). All the mice were injected intravenously daily for 7 days continuously and their body weight were recorded every day. Blood and urine samples were collected at day-8 then were used for further analysis. The mice were sacrificed and their organs including kidney, brain, and spinal cord were collected immediately.

To determine nephrotoxicity induced by colistin and colistin ABC-micelles, the blood samples were centrifuged at 4 °C and were analyzed with biochemical kits of neutrophils gelatinase-associated lipid delivery proteins (NGAL), BUN, and creatinine (CREA) purchased from mlbio (Shanghai, China) according to the protocols provided. The urine samples were centrifuged at 4 °C and were analyzed with biochemical kit of kidney injury molecule-1 (KIM-1) purchased from Solarbio (Beijing, China).

**Neurotoxicity of Free Colistin and Colistin ABC-Micelles in Vivo.** To determine neurotoxicity induced by colistin and colistin ABC-micelles, the function of the mitochondrial tissue and oxidative stress level of the brain homogenate were assessed as follows. The mitochondria were isolated from the brain tissue and spinal cord tissue, respectively, using a mitochondrial isolation kit (purchased from biyotime, Shanghai, China). Changes of a mitochondrial membrane potential were determined according to ref 56. Activities of the mitochondrial respiratory chain were detected according to a previously published literature<sup>56</sup> with minor modification. Briefly, isolated mitochondrial (8–10 mg protein) was mixed with 0.2 mL of excess methyl thiazolyl tetrazolium (MTT, 0.1 mg/mL), then dissolved in potassium chloride buffer (125 mM KCl, 2 mM  $K_2HPO_4$ , 1 mM  $MgCl_2$ , and 20 mM HEPES, adjusted to pH 7.4 with KOH), and incubated at 37 °C for 30 min, then subjected to centrifugation at 1000 rcf for 5 min at room temperature for formazan pellet. Then, the pellet was dissolved in 0.1 mL isopropanol, and absorbance was measured at 595 nm. As for oxidative stress of mice, catalase activity was detected according to a previously published protocol.<sup>19</sup> Briefly, the reaction mixture containing 0.1 mL of homogenate of the brain and 1 mL of hydrogen peroxide ( $H_2O_2$ , 20 mmol/L) was incubated at 37 °C for 3 min and 4 mL ammonium molybdate (32.4 mmol/L) was used as stopping reagents. The absorbance at 374 nm was measured immediately using a microplate reader. Caspase-3 level of brain homogenates was determined by caspase-3 kit purchased from mlbio (Shanghai, China). Beam score experiment: Neurobehavioral damage was evaluated by narrow beam score experiment according to previously reported reference with minor modifications.<sup>19</sup> A wooden beam with a length of 150 cm and diameter of 6 mm was used and divided into three parts. Each part is 50 cm and the beam was placed 60 cm above the floor. Scores of 0, 1, 2, and 3 were recorded after the mice crossed the narrow beam. The score of the mice that fell in the first part ( $d < 50$  cm,  $d$  is the distance that mouse moved on the beam before it fell), in the second part ( $50 < d < 100$  cm), in the third part ( $100 < d < 150$  cm), and crossed the beam without falling were scored as 0, 1, 2, and 3,

respectively. Histology experiments: organs of the kidney and brain were immersed in 10% formalin solution and fixed over 24 h. The fixed organs were immersed with increasing grade of alcohol, xylene, embedded in paraffin and then stained with hematoxylin and eosin stains. Subsequently, the slides were imaged by a microscope.

**In Vivo Treatment of Sepsis Mice Infected by MDR *E. coli* Bacteria.** Mice (CD-1, 8 weeks, female) were intraperitoneally injected with cyclophosphamide at a dose of 100 mg/kg for three consecutive days, then WBCs and lymphocyte (LYMs) were counted using a hemocytometer and Wright-Giemsa stain protocol, respectively. After the immunocompromised state was established, mice were infected with 0.1 mL of bacterial (strain MDR *E. coli*. ATCC BAA-2452, bio/wb, resistant to imipenem and ertapenem) suspension in PBS ( $2.5 \times 10^9$  CFUs/mL) by intravenous tail injection. After 2 h infection of bacteria, mice were left untreated or treated (i.v.) with free colistin, colistin ABC-micelles, and colistin-rifampicin-ABC micelles (CR-ABCs) with 3 mg/kg of colistin, respectively. After 24 h of bacterial infection, blood was collected through a facial vein. CFUs of mice were counted using the plate dilution colony method until the next day after incubation overnight. For the organ burden and interleukin-6 (IL-6) experiments, mice were given intravenously by different drug-formations for 3 days, and then were sacrificed and major organs and serum were collected for the measurement of bacterial burden in the organs and interleukin-6 (IL-6) level in the serum. For the experiments in Figure 4C–F, mice are treated by various colistin formulations based on 3 mg (colistin)/kg every other day. Meanwhile, survival rate and body weight (BW) were monitored closely every day. The 20% loss of BW or death was used as the early removal criteria for the calculation of survival rate.

**Pharmacokinetics and Biodistribution of Free Colistin and Colistin ABC-Micelles.** To label colistin with fluorescent dye of FITC, 2.8 mg of FITC in 300  $\mu$ L of DMSO was added dropwise to 10 mg of colistin (molar ratio of FITC to colistin is 1) in pH = 10 carbonate buffer solution and then stirred overnight. Colistin-FITC conjugate (COL-FITC) was quantified using the TNBSA method. After fluorescently labeling, as low as 0.05  $\mu$ g/mL can be detected with a linear relation of 0.999. To prepare colistin-FITC ABC-micelles, COL-FITC powder was freeze dried and dissolved in 100  $\mu$ L of DD water, then added dropwise to NPC-F127 sodium phosphate buffer solution as described above. Unconjugated molecules were removed by ultracentrifugation. To determine half-life in blood and biodistributions in major organs, colistin formations with a dose of 3 mg (colistin)/kg were injected intravenously via the tail vein. In addition, the blood was collected at indicated time points. Colistin was extracted using the mixture of distilled water and acetonitrile (7:3, v/v) before being subject to quantification. After 24 h of colistin injections, organs of the heart, liver, spleen, lung, kidney, and brain were collected and homogenized in the mixture of saline and acetonitrile (7:3, v/v). Centrifuge at 5400 rcf at 4 °C was conducted and supernatant was collected for the measurement of colistin concentration using the fluorescence labeling method. For fluorescent imaging of organs as shown in Figure 5D, mice are intravenously given FITC-labeled free colistin or colistin ABC-micelles with 5 mg (colistin)/kg. Twenty-four h after injection, mice were sacrificed and organs were collected and then imaged by IVIS (Night OWL II LB 983, Berthold technologies) with excitation/emission wavelengths at 485/520 nm.

**Microscopic Imaging of Bacteria Treated with Free Colistin or Colistin ABC-Micelles.** *P. aeruginosa* wild-type (WT) strain PAO1 was used. Strains were grown on LB agar (LB, 10 g/liter tryptone, 5 g/liter yeast extract, 5 g/liter NaCl) plates at 37 °C for 12 h. A single colony was transferred to a test tube containing 5 mL of liquid LB and cultured for 8 h to the logarithmic growth phase, with shaking at 220 rpm and 37 °C to an optical density at 600 nm (OD 600) of 3.0. Cultures were then diluted to an OD 600 of 0.05 in LB medium, which was then injected into a flow chamber assembled by attaching a cover glass as the substratum.

Ibidi flow cells made of polycarbonate were produced in Germany. Each flow cell has six identical rectangle channels (17 mm by 3.8 mm by 0.4 mm) and was assembled by attaching a cover glass as the substratum. The system was flushed for 5 min at a flow rate of 20 mL/h by LB medium using a syringe pump (Harvard Apparatus). Then, the

medium flow was stopped and 1 mL of a diluted bacterial culture (OD<sub>600</sub> of 0.05) was injected directly into the channel of the flow cell. After standing for 2 min, the floating cells were washed away by 20 mL/h LB flow. The remaining adherent cells grew and divided for 1 h at 30 °C using a flow rate of 0.5 mL/h of LB. Then, the flow rate was stopped, the rubber tube was clamped and a fixed concentration of free colistin or colistin ABC-micelles or shell fluorescently labeled with a dye of FITC were injected. Bright-field/FITC channels were used to capture the images at the indicated time point with at least three repeated shooting. Briefly, images were acquired using an electron-multiplying charge-coupled-device camera (Andor iXon Ultra 888). Bright-field images were obtained at 3 s intervals for a total of approximately 2.5 h, and the image size was 66.5 μm by 66.5 μm (10,241,024 pixels). Fluorescence pictures of drug-cell were collected with a fluoresceine isothiocyanate (FITC) filter, with an exposure time of 300 ms at 1 min intervals. The morphology changes of cells treated with various drug formations were statistically monitored and length of cells were recorded using MATLAB. The Z value was collected through adjusting the focal plane at a space of 0.05 μm from low to high after the treatment of free colistin and colistin ABC-micelles for 6 min. To study the interaction of the shell of ABC-micelles with cells, the shell was incubated with *P. aeruginosa* for 60 min and FITC was used to label colistin. For live/dead staining of cells, after incubating free colistin with cells for 10 and 90 min, drugs were washed away before injecting 300 μL of dye (LIVE/DEAD BacLight Bacterial Viability kit (L-7012; Molecular Probes, Eugene, OR, USA), followed by incubation in the dark chamber for 15 min. Then, images were captured immediately after washing away excess dyes.

## ■ ASSOCIATED CONTENT

### SI Supporting Information

The Supporting Information is available free of charge at <https://pubs.acs.org/doi/10.1021/acsami.0c21459>.

Material and reagents; Characterization of NPC-F127 and ABC-micelles, including NMR, yield, standard curves, parameters and stability; MIC and MBC data; toxicity, as well as hematoxylin and eosin-stained section and MTDs; CFUs and inflammatory biomarker of sepsis model; and microscopy imaging and movies (PDF)

Movie 1: Real-time imaging of bacteria treated by 16 μg/mL colistin ABC-micelles with rapid change of morphology (AVI)

Movie 2: Real-time imaging of bacteria treated by colistin with no significant morphology change (AVI)

Movie 3: Real-time imaging of bacteria treated by 32 μg/mL colistin ABC-micelles with rapid change of morphology (AVI)

## ■ AUTHOR INFORMATION

### Corresponding Authors

**Kun Zhao** – School of Chemical Engineering and Technology and Key Laboratory of Systems Bioengineering (Ministry of Education), Tianjin University, Tianjin 300350, P. R. China; [orcid.org/0000-0003-3928-1981](https://orcid.org/0000-0003-3928-1981); Email: [kunzhao@tju.edu.cn](mailto:kunzhao@tju.edu.cn)

**Jonathan F. Lovell** – Department of Biomedical Engineering, The State University of New York at Buffalo, Buffalo, New York 14260, United States; Email: [jflovell@buffalo.edu](mailto:jflovell@buffalo.edu)

**Yumiao Zhang** – School of Chemical Engineering and Technology and Key Laboratory of Systems Bioengineering (Ministry of Education), Tianjin University, Tianjin 300350, P. R. China; [orcid.org/0000-0002-6166-0470](https://orcid.org/0000-0002-6166-0470); Email: [ymzhang88@tju.edu.cn](mailto:ymzhang88@tju.edu.cn)

## Authors

**Xingyue Yang** – School of Chemical Engineering and Technology and Key Laboratory of Systems Bioengineering (Ministry of Education), Tianjin University, Tianjin 300350, P. R. China

**He Ren** – School of Chemical Engineering and Technology and Key Laboratory of Systems Bioengineering (Ministry of Education), Tianjin University, Tianjin 300350, P. R. China

**Hong Zhang** – School of Chemical Engineering and Technology and Key Laboratory of Systems Bioengineering (Ministry of Education), Tianjin University, Tianjin 300350, P. R. China

**Gengqi Liu** – School of Chemical Engineering and Technology and Key Laboratory of Systems Bioengineering (Ministry of Education), Tianjin University, Tianjin 300350, P. R. China

**Zhen Jiang** – School of Chemical Engineering and Technology and Key Laboratory of Systems Bioengineering (Ministry of Education), Tianjin University, Tianjin 300350, P. R. China

**Qian Qiu** – School of Chemical Engineering and Technology and Key Laboratory of Systems Bioengineering (Ministry of Education), Tianjin University, Tianjin 300350, P. R. China

**Cui Yu** – School of Chemical Engineering and Technology and Key Laboratory of Systems Bioengineering (Ministry of Education), Tianjin University, Tianjin 300350, P. R. China

**Niren Murthy** – Department of Bioengineering, University of California Berkeley, Berkeley, California 94720, United States

Complete contact information is available at:

<https://pubs.acs.org/doi/10.1021/acsami.0c21459>

## Author Contributions

X.Y. and Y.Z. conceived the project. X.Y. carried out most experiments. H.R., Q.Q. and C.Y. assisted with animal experiments. G.L. and Z.J. assisted with material synthesis and characterization. H.Z. and K.Z. designed and conducted the experiments of microscopic imaging of bacteria. X.Y., N.M., K.Z., J.F.L. and Y.Z. performed data analysis and wrote the manuscript.

## Funding

This work is supported by the Start-Up grant at Tianjin University (Y.Z.) and One-thousand Young Talent Program (Y.Z.), the National Key R&D Program of China (2018YFA0902102 to K.Z.), and the National Natural Science Foundation of China (32071384 to Y.Z.; 21621004 to K.Z.).

## Notes

The authors declare no competing financial interest.

## ■ ACKNOWLEDGMENTS

We thank Professor Lei Zhang for the assistance with DLS measurement.

## ■ ABBREVIATION

ABC-micelles, antibiotic crosslinked micelles  
CR-ABC, colistin-rifampicin co-loaded antibiotic crosslinked micelles  
BUN, blood urea nitrogen  
CREA, creatinine  
NGAL, neutrophil gelatinase-associated lipocalin  
KIM-1, kidney injury molecule-1  
MMP, mitochondrial membrane potential  
MRC, mitochondrial respiratory chain  
IL-6, interleukin-6

## REFERENCES

- (1) Travis, J. Reviving the Antibiotic Miracle? *Science* **1994**, *264*, 360.
- (2) Wilmes, D.; Coche, E.; Rodriguez-Villalobos, H.; Kanaan, N. Bacterial Pneumonia in Kidney Transplant Recipients. *Respir. Med.* **2018**, *137*, 89–94.
- (3) Kwon, E. J.; Skalak, M.; Bertucci, A.; Braun, G.; Ricci, F.; Ruoslahti, E.; Sailor, M. J.; Bhatia, S. N. Silicon Nanoparticles: Porous Silicon Nanoparticle Delivery of Tandem Peptide Anti-Infectives for the Treatment of Pseudomonas Aeruginosa Lung Infections. *Adv. Mater.* **2017**, *29*, 35.
- (4) Lemichez, E.; Lecuit, M.; Nassif, X.; Bourdoulous, S. Breaking the Wall: Targeting of the Endothelium by Pathogenic Bacteria. *Nat. Rev. Microbiol.* **2010**, *8*, 93–104.
- (5) Klein, R. D.; Hultgren, S. J. Urinary Tract Infections: Microbial Pathogenesis, Host-Pathogen Interactions and New Treatment Strategies. *Nat. Rev. Microbiol.* **2020**, *18*, 211–226.
- (6) Lin, Y.-W.; Chen, K.; Wang, J.; Velkov, T.; Zhou, Q. T.; Li, J. A Proof-of-Concept Study of the Efficacy of Systemically Administered Polymyxins in Mouse Burn Wound Infection Caused by Multidrug-Resistant Gram-Negative Pathogens. *Antimicrob. Agents Chemother.* **2018**, *62*, No. e02527.
- (7) Zhang, C. Y.; Gao, J.; Wang, Z. Bioresponsive Nanoparticles Targeted to Infectious Microenvironments for Sepsis Management. *Adv. Mater.* **2018**, *30*, 1803618.
- (8) Mao, D.; Hu, F.; Kenry, J. S.; Wu, W.; Ding, D.; Kong, D.; Liu, B. Metal-Organic-Framework-Assisted In Vivo Bacterial Metabolic Labeling and Precise Antibacterial Therapy. *Adv. Mater.* **2018**, *30*, 1706831.
- (9) Song, Z.; Wu, Y.; Cao, Q.; Wang, H.; Wang, X.; Han, H. pH-Responsive, Light-Triggered on-Demand Antibiotic Release from Functional Metal-Organic Framework for Bacterial Infection Combination Therapy. *Adv. Funct. Mater.* **2018**, *28*, 1800011.
- (10) Kim, T.; Zhang, Q.; Li, J.; Zhang, L.; Jokerst, J. V. A Gold/Silver Hybrid Nanoparticle for Treatment and Photoacoustic Imaging of Bacterial Infection. *ACS Nano* **2018**, *12*, 5615–5625.
- (11) Gao, W.; Chen, Y.; Zhang, Y.; Zhang, Q.; Zhang, L. Nanoparticle-Based Local Antimicrobial Drug Delivery. *Adv. Drug Delivery Rev.* **2018**, *127*, 46–57.
- (12) Pompattananangkul, D.; Zhang, L.; Olson, S.; Aryal, S.; Obonyo, M.; Vecchio, K.; Huang, C.-M.; Zhang, L. Bacterial Toxin-Triggered Drug Release from Gold Nanoparticle-Stabilized Liposomes for the Treatment of Bacterial Infection. *J. Am. Chem. Soc.* **2011**, *133*, 4132–4139.
- (13) Willyard, C. The Drug-Resistant Bacteria That Pose the Greatest Health Threats. *Nature* **2017**, *543*, 15.
- (14) Falagas, M. E.; Kasiakou, S. K.; Saravolatz, L. D. Colistin: The Revival of Polymyxins for the Management of Multidrug-Resistant Gram-Negative Bacterial Infections. *Clin. Infect. Dis.* **2005**, *40*, 1333–1341.
- (15) Chen, L.-K.; Kuo, S.-C.; Chang, K.-C.; Cheng, C.-C.; Yu, P.-Y.; Chang, C.-H.; Chen, T.-Y.; Tseng, C.-C. Clinical Antibiotic-Resistant Acinetobacter Baumannii Strains with Higher Susceptibility to Environmental Phages than Antibiotic-Sensitive Strains. *Sci. Rep.* **2017**, *7*, 6319.
- (16) Levy-Blitchein, S.; Roca, I.; Plasencia-Rebata, S.; Vicente-Taboada, W.; Velázquez-Pomar, J.; Muñoz, L.; Moreno-Morales, J.; Pons, M. J.; Del Valle-Mendoza, J.; Vila, J. Emergence and Spread of Carbapenem-Resistant Acinetobacter Baumannii International Clones II and III in Lima, Peru. *Emerg. Microb. Infect.* **2018**, *7*, 119.
- (17) Nowak, J.; Zander, E.; Stefanik, D.; Higgins, P. G.; Roca, I.; Vila, J.; McConnell, M. J.; Cisneros, J. M.; Seifert, H. High Incidence of Pandrug-Resistant Acinetobacter Baumannii Isolates Collected from Patients with Ventilator-Associated Pneumonia in Greece, Italy and Spain as Part of the MagicBullet Clinical Trial. *J. Antimicrob. Chemother.* **2017**, *72*, 3277–3282.
- (18) Ozyilmaz, E.; Ebinc, F. A.; Derici, U.; Gulbahar, O.; Goktas, G.; Elmas, C.; Oguzulgen, I. K.; Sindel, S. Could Nephrotoxicity Due to Colistin Be Ameliorated with the Use of N-Acetylcysteine? *Intensive Care Med.* **2011**, *37*, 141–146.
- (19) To, A. Colistin Sulphate Induced Neurotoxicity: Studies on Cholinergic, Monoaminergic, Purinergic and Oxidative Stress Biomarkers. *Biomed. Pharmacother.* **2018**, *103*, 1701–1707.
- (20) Evans, M. E.; Feola, D. J.; Rapp, R. P. Polymyxin B Sulfate and Colistin: Old Antibiotics for Emerging Multiresistant Gram-Negative Bacteria. *Ann. Pharmacother.* **1999**, *33*, 960–967.
- (21) Li, Z.; Velkov, T. Polymyxins: Mode of Action. *Adv. Exp. Med. Biol.* **2019**, *1145*, 37–54.
- (22) Price, D. J. E.; Graham, D. I. Effects of Large Doses of Colistin Sulphomethate Sodium on Renal Function. *Br. Med. J.* **1970**, *4*, 525–527.
- (23) Dai, C.; Ciccotosto, G. D.; Cappai, R.; Wang, Y.; Tang, S.; Hoyer, D.; Schneider, E. K.; Velkov, T.; Xiao, X. Rapamycin Confers Neuroprotection against Colistin-Induced Oxidative Stress, Mitochondria Dysfunction, and Apoptosis through the Activation of Autophagy and MTOR/Akt/CREB Signaling Pathways. *ACS Chem. Neurosci.* **2018**, *9*, 824–837.
- (24) Dai, C.; Xiao, X.; Li, J.; Ciccotosto, G. D.; Cappai, R.; Tang, S.; Schneider-Futschik, E. K.; Hoyer, D.; Velkov, T.; Shen, J. Molecular Mechanisms of Neurotoxicity Induced by Polymyxins and Chemoprevention. *ACS Chem. Neurosci.* **2019**, *10*, 120–131.
- (25) Pohlmann, G. Respiratory Arrest Associated with Intravenous Administration of Polymyxin B Sulfate. *J. Am. Med. Assoc.* **1966**, *196*, 181–183.
- (26) Bergen, P. J.; Li, J.; Rayner, C. R.; Nation, R. L. Colistin Methanesulfonate Is an Inactive Prodrug of Colistin against Pseudomonas Aeruginosa. *Antimicrob. Agents Chemother.* **2006**, *50*, 1953–1958.
- (27) Wallace, S. J.; Li, J.; Nation, R. L.; Pranker, R. J.; Boyd, B. J. Interaction of Colistin and Colistin Methanesulfonate with Liposomes: Colloidal Aspects and Implications for Formulation. *J. Pharm. Sci.* **2012**, *101*, 3347–3359.
- (28) Li, J.; Milne, R. W.; Nation, R. L.; Turnidge, J. D.; Coulthard, K. Stability of Colistin and Colistin Methanesulfonate in Aqueous Media and Plasma as Determined by High-Performance Liquid Chromatography. *Antimicrob. Agents Chemother.* **2003**, *47*, 1364–1370.
- (29) Nation, R. L.; Li, J.; Cars, O.; Couet, W.; Dudley, M. N.; Kaye, K. S.; Mouton, R. W.; Paterson, D. L.; Tam, V. H.; Theuretzbacher, U.; Tsuji, B. T.; Turnidge, J. D. Framework for Optimisation of the Clinical Use of Colistin and Polymyxin B: The Prato Polymyxin Consensus. *Lancet Infect. Dis.* **2015**, *15*, 225–234.
- (30) Metcalf, A. P.; Hardaker, L. E. A.; Hatley, R. H. M. A Simple Method for Assaying Colistimethate Sodium in Pharmaceutical Aerosol Samples Using High Performance Liquid Chromatography. *J. Pharm. Biomed. Anal.* **2017**, *142*, 15–18.
- (31) Varache, M.; Powell, L. C.; Aarstad, O. A.; Williams, T. L.; Wenzel, M. N.; Thomas, D. W.; Ferguson, E. L. Polymer Masked-Unmasked Protein Therapy: Identification of the Active Species after Amylase Activation of Dextrin-Colistin Conjugates. *Mol. Pharm.* **2019**, *16*, 3199–3207.
- (32) Roberts, J. L.; Cattoz, B.; Schweins, R.; Beck, K.; Thomas, D. W.; Griffiths, P. C.; Ferguson, E. L. In Vitro Evaluation of the Interaction of Dextrin-Colistin Conjugates with Bacterial Lipopolysaccharide. *J. Med. Chem.* **2016**, *59*, 647–654.
- (33) Ferguson, E. L.; Azzopardi, E.; Roberts, J. L.; Walsh, T. R.; Thomas, D. W. Dextrin-Colistin Conjugates as a Model Bioresponsive Treatment for Multidrug Resistant Bacterial Infections. *Mol. Pharm.* **2014**, *11*, 4437–4447.
- (34) Liu, Y.; Ren, Y.; Li, Y.; Su, L.; Zhang, Y.; Huang, F.; Liu, J.; Liu, J.; van Kooten, T. G.; An, Y.; Shi, L.; van der Mei, H. C.; Busscher, H. J. Nanocarriers with Conjugated Antimicrobials to Eradicate Pathogenic Biofilms Evaluated in Murine In Vivo and Human Ex Vivo Infection Models. *Acta Biomater.* **2018**, *79*, 331–343.
- (35) Gounani, Z.; Asadollahi, M. A.; Meyer, R. L.; Arpanaei, A. Loading of Polymyxin B onto Anionic Mesoporous Silica Nanoparticles Retains Antibacterial Activity and Enhances Biocompatibility. *Int. J. Pharm.* **2018**, *537*, 148–161.
- (36) Carrillo-Carrión, C.; Simonet, B. M.; Valcárcel, M. Colistin-Functionalised CdSe/ZnS Quantum Dots as Fluorescent Probe for the

Rapid Detection of Escherichia Coli. *Biosens. Bioelectron.* **2011**, *26*, 4368–4374.

(37) Chai, G.; Park, H.; Yu, S.; Zhou, F.; Li, J.; Xu, Q.; Zhou, Q. Evaluation of Co-Delivery of Colistin and Ciprofloxacin in Liposomes Using an in Vitro Human Lung Epithelial Cell Model. *Int. J. Pharm.* **2019**, *569*, 118616.

(38) Liu, Y.-H.; Kuo, S.-C.; Yao, B.-Y.; Fang, Z.-S.; Lee, Y.-T.; Chang, Y.-C.; Chen, T.-L.; Hu, C.-M. J. Colistin Nanoparticle Assembly by Coacervate Complexation with Polyanionic Peptides for Treating Drug-Resistant Gram-Negative Bacteria. *Acta Biomater.* **2018**, *82*, 133–142.

(39) Hou, X.; Zhang, X.; Zhao, W.; Zeng, C.; Deng, B.; McComb, D. W.; Du, S.; Zhang, C.; Li, W.; Dong, Y. Vitamin Lipid Nanoparticles Enable Adoptive Macrophage Transfer for the Treatment of Multidrug-Resistant Bacterial Sepsis. *Nat. Nanotechnol.* **2020**, *15*, 41–46.

(40) Azad, M. A. K.; Sivanesan, S.; Wang, J.; Chen, K.; Nation, R. L.; Thompson, P. E.; Roberts, K. D.; Velkov, T.; Li, J. Methionine Ameliorates Polymyxin-Induced Nephrotoxicity by Attenuating Cellular Oxidative Stress. *Antimicrob. Agents Chemother.* **2017**, *62*, No. e01254.

(41) Sivanesan, S. S.; Azad, M. A. K.; Schneider, E. K.; Ahmed, M. U.; Huang, J.; Wang, J.; Li, J.; Nation, R. L.; Velkov, T. Gelofusine Ameliorates Colistin-Induced Nephrotoxicity. *Antimicrob. Agents Chemother.* **2017**, *61*, No. e00985.

(42) Dai, C.; Tang, S.; Deng, S.; Zhang, S.; Zhou, Y.; Velkov, T.; Li, J.; Xiao, X. Lycopene Attenuates Colistin-Induced Nephrotoxicity in Mice via Activation of the Nrf2/HO-1 Pathway. *Antimicrob. Agents Chemother.* **2015**, *59*, 579–585.

(43) Yousef, J. M.; Chen, G.; Hill, P. A.; Nation, R. L.; Li, J. Ascorbic Acid Protects against the Nephrotoxicity and Apoptosis Caused by Colistin and Affects Its Pharmacokinetics. *J. Antimicrob. Chemother.* **2012**, *67*, 452–459.

(44) Dai, C.; Ciccosto, G. D.; Cappai, R.; Tang, S.; Li, D.; Xie, S.; Xiao, X.; Velkov, T. Curcumin Attenuates Colistin-Induced Neurotoxicity in N2a Cells via Anti-inflammatory Activity, Suppression of Oxidative Stress, and Apoptosis. *Mol. Neurobiol.* **2018**, *55*, 421–434.

(45) Li, Z.-D.; Luo, J.; Jia, L.-H.; Wang, X.-Y.; Xun, Z.-K.; Liu, M. Cytochrome C Suppresses Renal Accumulation and Nephrotoxicity of Polymyxin B. *Hum. Exp. Toxicol.* **2019**, *38*, 193–200.

(46) Ye, X.; Zhang, J.; Chen, H.; Wang, X.; Huang, F. Fluorescent Nanomicelles for Selective Detection of Sudan Dye in Pluronic F127 Aqueous Media. *ACS Appl. Mater. Interfaces* **2014**, *6*, 5113–5121.

(47) Kong, W. H.; Lee, W. J.; Cui, Z. Y.; Bae, K. H.; Park, T. G.; Kim, J. H.; Park, K.; Seo, S. W. Nanoparticulate Carrier Containing Water-Insoluble Iodinated Oil as a Multifunctional Contrast Agent for Computed Tomography Imaging. *Biomaterials* **2007**, *28*, 5555–5561.

(48) Shriky, B.; Kelly, A.; Isreb, M.; Babenko, M.; Mahmoudi, N.; Rogers, S.; Shebanova, O.; Snow, T.; Gough, T. Pluronic F127 Thermosensitive Injectable Smart Hydrogels for Controlled Drug Delivery System Development. *J. Colloid Interface Sci.* **2020**, *565*, 119–130.

(49) Zhang, Y.; Song, W.; Geng, J.; Chitgupi, U.; Unsal, H.; Federizon, J.; Rzyayev, J.; Sukumaran, D. K.; Alexandridis, P.; Lovell, J. F. Therapeutic Surfactant-Stripped Frozen Micelles. *Nat. Commun.* **2016**, *7*, 11649.

(50) Smith, P. K.; Krohn, R. I.; Hermanson, G. T.; Mallia, A. K.; Gartner, F. H.; Provenzano, M. D.; Fujimoto, E. K.; Goeke, N. M.; Olson, B. J.; Klenk, D. C. Measurement of Protein Using Bicinchoninic Acid. *Anal. Biochem.* **1985**, *150*, 76–85.

(51) Lee, H. J.; Bergen, P. J.; Bulitta, J. B.; Tsuji, B.; Forrest, A.; Nation, R. L.; Li, J. Synergistic Activity of Colistin and Rifampin Combination against Multidrug-Resistant *Acinetobacter baumannii* in an In Vitro Pharmacokinetic/Pharmacodynamic Model. *Antimicrob. Agents Chemother.* **2013**, *57*, 3738–3745.

(52) Li, J.; Milne, R. W.; Nation, R. L.; Turnidge, J. D.; Smeaton, T. C.; Coulthard, K. Use of High-Performance Liquid Chromatography to Study the Pharmacokinetics of Colistin Sulfate in Rats Following Intravenous Administration. *Antimicrob. Agents Chemother.* **2003**, *47*, 1766–1770.

(53) Huang, J.; Li, J.; Lyu, Y.; Miao, Q.; Pu, K. Molecular Optical Imaging Probes for Early Diagnosis of Drug-Induced Acute Kidney Injury. *Nat. Mater.* **2019**, *18*, 1133–1143.

(54) Cheng, P.; Miao, Q.; Huang, J.; Li, J.; Pu, K. Multiplex Optical Urinalysis for Early Detection of Drug-Induced Kidney Injury. *Anal. Chem.* **2020**, *92*, 6166–6172.

(55) Dai, C.; Tang, S.; Biao, X.; Xiao, X.; Chen, C.; Li, J. Colistin Induced Peripheral Neurotoxicity Involves Mitochondrial Dysfunction and Oxidative Stress in Mice. *Mol. Biol. Rep.* **2019**, *46*, 1963–1972.

(56) Dai, C.; Li, J.; Li, J. New Insight in Colistin Induced Neurotoxicity with the Mitochondrial Dysfunction in Mice Central Nervous Tissues. *Exp. Toxicol. Pathol.* **2013**, *65*, 941–948.

(57) Prasad, S. N.; Muralidhara. Neuroprotective Efficacy of Eugenol and Isoeugenol in Acrylamide-Induced Neuropathy in rats: Behavioral and Biochemical evidence. *Neurochem. Res.* **2013**, *38*, 330–345.

(58) Chelikani, P.; Fita, I.; Loewen, P. C. Diversity of Structures and Properties among Catalases. *Cell. Mol. Life Sci.* **2004**, *61*, 192–208.

(59) Kang, M. Y.; Kim, H.-B.; Piao, C.; Lee, K. H.; Hyun, J. W.; Chang, I.-Y.; You, H. J. The Critical Role of Catalase in Prooxidant and Antioxidant Function of P53. *Cell Death Differ.* **2013**, *20*, 117–129.

(60) Busscher, H. J.; Woudstra, W.; van Kooten, T. G.; Jutte, P.; Shi, L.; Liu, J.; Hinrichs, W. L. J.; Frijlink, H. W.; Shi, R.; Liu, J.; Parvizi, J.; Kates, S.; Rotello, V. M.; Schaer, T. P.; Williams, D.; Grainger, D. W.; van der Mei, H. C. Accepting Higher Morbidity in Exchange for Sacrificing Fewer Animals in Studies Developing Novel Infection-Control Strategies. *Biomaterials* **2020**, *232*, 119737.

(61) Zhang, W.; Wang, Y.; Lu, H.; Liu, Q.; Wang, C.; Hu, W.; Zhao, K. Dynamics of Solitary Predation by *Myxococcus Xanthus* on *Escherichia Coli* Observed at the Single-Cell Level. *Appl. Environ. Microbiol.* **2020**, *86*, e02286–19.

(62) Mortensen, N. P.; Fowlkes, J. D.; Sullivan, C. J.; Allison, D. P.; Larsen, N. B.; Molin, S.; Doktycz, M. J. Effects of Colistin on Surface Ultrastructure and Nanomechanics of *Pseudomonas Aeruginosa* Cells. *Langmuir* **2009**, *25*, 3728–3733.

(63) Koike, M.; Iida, K.; Matsuo, T. Electron Microscopic Studies on Mode of Action of Polymyxin. *J. Bacteriol.* **1969**, *97*, 448–452.

(64) Ayoub Moubareck, C. Polymyxins and Bacterial Membranes: A Review of Antibacterial Activity and Mechanisms of Resistance. *Membranes* **2020**, *10*, 181.

(65) Zhang, Y.; Jeon, M.; Rich, L. J.; Hong, H.; Geng, J.; Zhang, Y.; Shi, S.; Barnhart, T. E.; Alexandridis, P.; Huiying, J. D.; Seshadri, M.; Cai, W.; Kim, C.; Lovell, J. F. Non-Invasive Multimodal Functional Imaging of the Intestine with Frozen Micellar Naphthalocyanines. *Nat. Nanotechnol.* **2014**, *9*, 631–638.

(66) Zhang, Y.; Wang, D.; Goel, S.; Sun, B.; Chitgupi, U.; Geng, J.; Sun, H.; Barnhart, T. E.; Cai, W.; Xia, J.; Lovell, J. F. Surfactant-Stripped Frozen Pheophytin Micelles for Multimodal Gut Imaging. *Adv. Mater.* **2016**, *28*, 8524–8530.